

SiO₂ 胶体晶体垂直沉积自组装方法的改进

张 焱^{*,1} 郝 琦¹ 冯一军¹ 陆春华² 许仲梓²

(¹ 南京大学电子科学与工程学院电子工程系, 南京 210093)

(² 南京工业大学材料科学与工程学院材料化学工程国家重点实验室, 南京 210009)

摘要: 采用垂直沉积技术及相应的改进方法, 使用化学合成的 400 nm 单分散二氧化硅微球自组装制备了胶体晶体薄膜。通过扫描电镜与分光光度计对样品的微观结构与透过光谱进行了表征, 并对比研究了不同的垂直沉积方法对胶体晶体的影响。结果表明, 通过温度与流量控制两种改进手段, 均能制备具有六方密堆结构周期排列的胶体晶体薄膜。在垂直沉积过程中适当的升高温度有利于降低胶体粒子的用量, 而通过流量控制的垂直沉积技术则可以有效缩短自组装时间。通过调节蠕动泵改变液面与基板的相对运动速度, 或者调控温度改变胶体溶液的蒸发速率, 可在材料表面形成单层或多层的胶体晶体薄膜。改进的垂直沉积技术将有望应用于快速沉积大面积、高质量的胶体晶体材料。

关键词: 自组装; 胶体晶体; 垂直沉积; 光学性能; SiO₂ 微球

中图分类号: O613.72; O648.12+1

文献标识码: A

文章编号: 1001-4861(2011)05-0935-08

Self-assembly of Silica Colloidal Crystals by Improved Vertical Deposition Methods

ZHANG Yan^{*,1} HAO Yu¹ FENG Yi-Jun¹ LU Chun-Hua² XU Zhong-Zi²

(¹ Department of Electronic Engineering, School of Electronic Science and Engineering,
Nanjing University, Nanjing, 210093 China)

(² State Key Laboratory of Materials-Oriented Chemical Engineering, College of Material Science and Engineering,
Nanjing University of Technology, Nanjing, 210009 China)

Abstract: The fabrication and characterization of silica colloidal crystal films self-assembled from suspension of monodisperse silica spheres are reported through different improvement on vertical deposition. Three vertical deposition methods on the crystal formation were compared in terms of microstructure and optical transmission measurements. The results show that both the temperature-controlled vertical deposition and the flow-controlled vertical deposition could gain closely packed structures as traditional method but with lower colloid consumption and shorter time of self-assembly. By adjusting the rate of solvent evaporation or the relative movement between the liquid-surface and substrate, it is possible to transfer monolayer or multilayer of silica colloidal crystals onto the substrates. The improved methods can be used for rapid deposition of high-quality colloidal crystal films over large surface area without any special equipment.

Key words: self-assembly; colloidal crystal; vertical deposition; optical property; silica spheres

0 Introduction

Colloidal crystals, which are regular crystalline

arrays made by monodisperse spheres of dielectric materials such as silica or polymers, have drawn a considerable interest in the field of materials chemistry,

收稿日期: 2010-12-03。收修改稿日期: 2010-01-18。

国家自然科学基金(No.60990320, 60990322, 60801001)资助项目。

*通讯联系人。E-mail: njyanzh@163.com

both for theoretical and experimental considerations. The unique optical properties enable them to have many applications in the microelectronic and optoelectronic materials and engineering, due to the peculiar light interactions with the periodicity nanostructure of the colloidal crystals^[1-4]. Numerous attempts have been made on fabricating high quality colloidal crystals with few crystalline defects^[5-10]. Among them, the self-assembling of the monodisperse microspheres to create three-dimensional (3D) opal structures is a simple and inexpensive approach^[11-15]. Various methods have been proposed in the literature^[16-22], in which the vertical deposition (VD) method has gained a great deal of attention, due to the convenience of operation.

The VD method is based on the strong attractive capillary force at a meniscus between a vertical flat surface and colloidal particles that can introduce the formation of crystalline colloidal multilayers. Although traditional vertical deposition technique requires no special equipment or training and offers a good control over structure defects, they are very time-consuming and often result in non-uniformity of the deposited film. Because the liquid surface is controlled by the solvent volatilization, the concentration of particles changes during evaporation, which may have an effect on the film thickness. Moreover, for a certain particle size (with diameter more than 0.4 μm)^[11], the sedimentation is faster than ethanol evaporation, and the self-assembly of particles sometimes fails to take place.

In the past few years, many researchers have investigated the conditions that lead to the optimal quality of colloidal crystals by VD, such as solvent surface tension and ionic strength^[23], substrate wettability^[24], chemical or thermal modification of the particles^[25-26]. To improve the applications of VD method, some modifications on the method have been described. Gu et al.^[27] described a device for the fabrication of opal films by lifting the substrate out of the colloidal suspension. Vlasov et al.^[11] introduced a temperature gradient to allow convective flow to minimize particle sedimentation. Another development was made by Zheng et al.^[28] in their concise pressure controlled isothermal heating VD method for fabricating

photonic crystals from polystyrene spheres.

Although many efforts have been devoted to control the deposition process in VD method, the film quality is far from the requirement for practical applications^[29]. Most studies are concerned mainly with the final crystal quality, rather than the crystal growth features at the meniscus. Therefore, improving the VD method to control the morphology and quality of the films are still challenging in the preparation of colloidal crystals. We report here the easy and relative rapid fabrication of 3D colloidal crystals with controllable quality via the improved VD technique. By increasing the rate of solvent evaporation or the relative movement between the liquid-surface and substrate, we fabricated silica colloidal crystals with controllable structures. The colloidal crystals quality and the optical properties were characterized with scanning electron microscope and UV-Vis-NIR spectroscopy.

1 Experimental

1.1 Silica particle synthesis

Colloidal SiO_2 nanospheres of diameter about 400 nm were synthesized following the Stöber-Fink-Bohn method^[30]. All solvents and chemicals were purchased at reagent grade and used without further purification. Nanospheres with different sizes are obtained through strict control of the reaction conditions^[31-32]. The polydispersity of microspheres used in this work is typically less than 0.05, measured by dynamic light-scattering (DLS) measurement using a Brookhaven Zeta PALS analyzer. The as-synthesized silica spheres were purified and redispersed in anhydrous ethanol by at least four centrifugation/redispersion cycles in order to remove impurities, such as ammonia, water, and unreacted TEOS.

1.2 Fabrication of Colloidal Crystal Films

Quartz glass substrates (40 mm \times 20 mm \times 1 mm) were cleaned with anhydrous ethanol and acetone for 20 min in an ultrasonic bath, respectively. Then, the substrate was pre-cleaned with piranha solution ($V_{\text{H}_2\text{SO}_4} : V_{\text{H}_2\text{O}_2} = 4:1$) at 80 $^\circ\text{C}$ for 10 min. After that, the substrates were rinsed with deionized water and dried in nitrogen gas flow before use. A clean quartz substrate, which is

hydrophilic after the treatment, was then placed vertically into 10 mL of purified silica suspension in a clean beaker, which was covered by a 1 000 mL beaker to keep out external airflow and contamination. The entire apparatus was placed in a temperature-controlled oven. In order to obtain the optimal growth condition, the evaporation rate was controlled by adjusting the temperature. To evaluate the effect of the evaporation rate on the film properties, the colloidal crystals were fabricated at different evaporation temperatures, named as temperature-controlled vertical deposition (TCVD). After complete evaporation of ethanol, iridescent colloidal crystal films were obtained on the quartz glass substrate. A large area (30×20 mm) sample can be made over 1~2 d. Colloids with volume fractions of 0.25%, 0.5%, 1.0% and 2.0% were used to determine their effect on the film properties.

Another improvement on the VD method, named as the flow-controlled vertical deposition (FCVD)^[33], was also carried out for the growth of colloidal crystals. The beaker containing SiO₂ colloidal suspension was withdrawn from the container by using a variable-flow peristaltic pump to control the liquid surface dropping velocity of the colloidal suspension. By maintaining a constant flow rate of the peristaltic pump, we could

fabricate colloidal spheres in large domains with a controllable thickness.

1.3 Characterization of colloidal crystal films

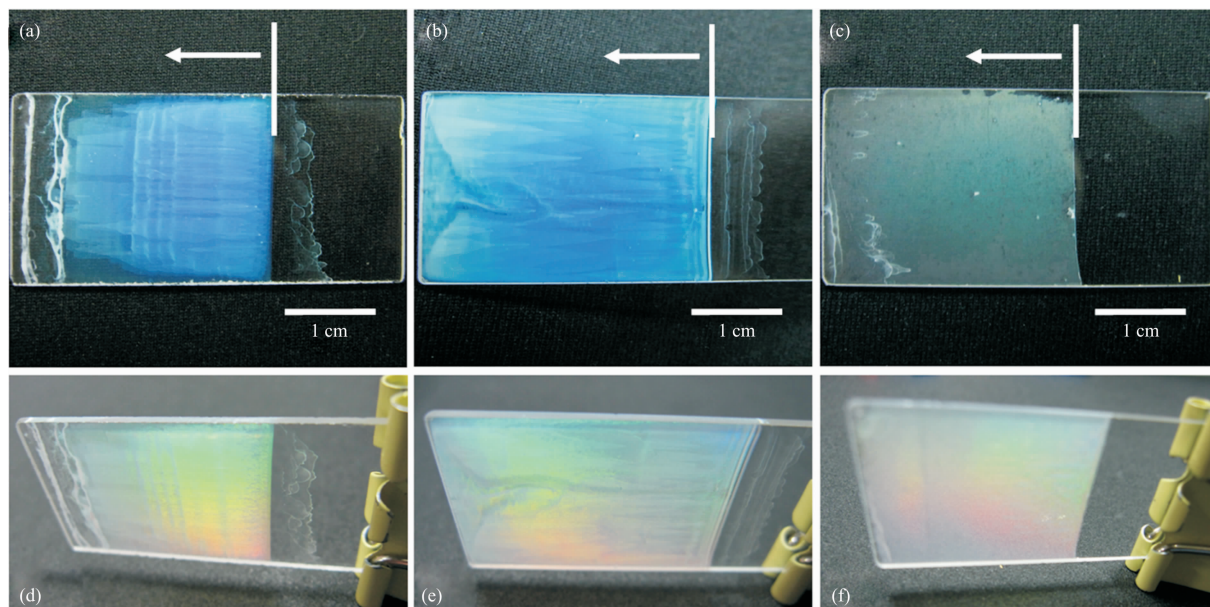
The microstructures of the SiO₂ colloidal crystal films, both top views and cross sections, were investigated using a Hitachi S-3400 scanning electron microscope (SEM) under an acceleration voltage of 30 kV. The samples for SEM observation were scraped by using a sharp razor blade and then sputtered with thin gold films. Optical transmission of the silica colloidal single crystal films were measured on a Shimadzu 3101PC UV-Vis-NIR spectrophotometer at normal incidence. The photographs of the colloidal crystal were taken using a digital camera (IXUS 870IS, Canon) under illumination of room light.

2 Results and discussion

2.1 Structural and morphological properties

2.1.1 Overviews

To improve long-range crystalline quality in colloidal self-assembly, the origins of macroscopic imperfections were analyzed during 3D colloidal crystal growth from the different vertical depositions. Fig.1(a)~(f) show overviews of the films prepared by the different VD methods. The white lines in the Fig.1 (a)~(c)



(a) NVD, (b) TCVD (55 °C), (c) FCVD (0.70 $\mu\text{m}\cdot\text{s}^{-1}$), (d-f) images show the optical features in oblique angle, respectively. The white lines show the initial level of immersion of the substrates, and the arrows in (a), (b) and (c) indicate the film growth direction

Fig.1 Overviews of the opal films made by the different VD methods from 400 nm SiO₂ with the same volume fraction (1.0%)

indicate roughly the immersion levels of the substrates upon insertion into the suspensions where the growth begins. As the Bragg diffraction peak for 400 nm SiO_2 nanospheres appears at near-infrared region under normal incidence light, the optical characteristic of the film can be judged with oblique incidence. A uniformly brilliant color that extends to centimeter dimensions can be observed for three films in oblique photographs, as shown in Fig.1(d)~(f).

Without the control of temperature and flow rate of the peristaltic pump, the natural VD (NVD) method usually leads to films that are not continuous and are separated into many individual grains and gaps (i.e. cracks). As observed in Fig.1 (a), the film becomes thinner and translucent with further growth. The film obtained this way shows a basically filmless area at the end of the growth direction. This naked area is caused by the sedimentation of larger SiO_2 nanospheres, which suggests that the NVD method is not suitable for large-scale assembly of colloidal photonic crystal with 400 nm SiO_2 nanospheres.

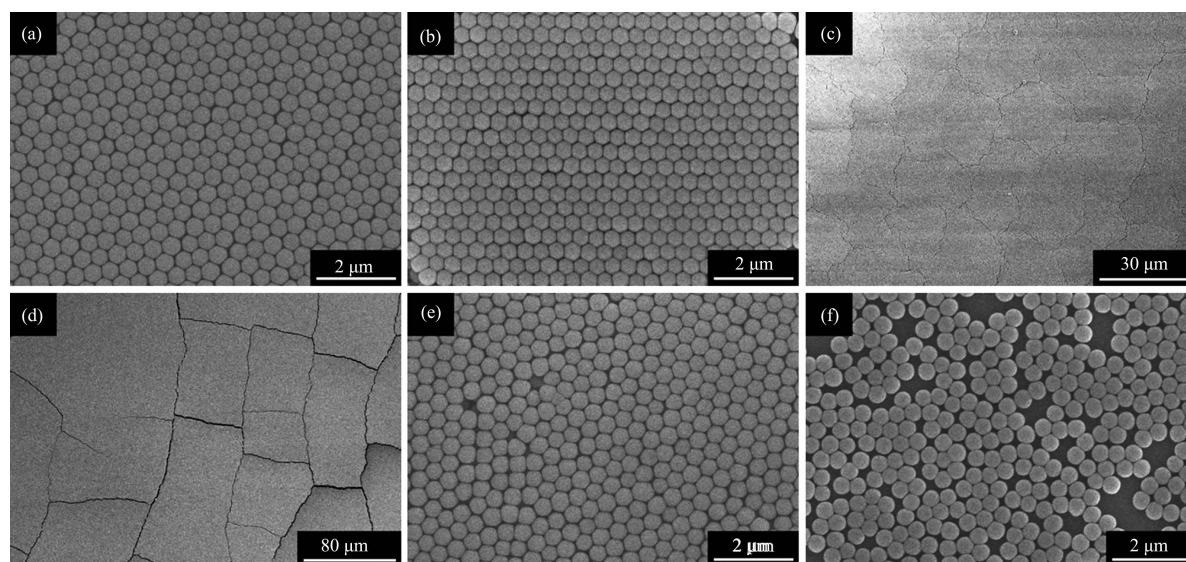
With the help of temperature control, a similar but more rapid process of crystal growth was obtained, as shown in Fig.1(b). The growth begins with the formation of bands parallel to the liquid/substrate interface. The film formed in the right region of white line is thin and visibly undulating with the evaporation of ethanol. Further along

the growth direction, the undulation ends and the film becomes opaque and more uniform in thickness, although very fine cracks running parallel to the growth direction can be seen. The growth of colloid film has been extended to the edge of the substrate as well as the periodic structure, which can be judged from Fig.1(e).

Fig.1 (c) shows the film deposited by FCVD on quartz glass substrate, which was dipped in the colloidal suspension and withdrawn at a rate of $0.70 \mu\text{m} \cdot \text{s}^{-1}$. During the growth of colloidal crystal, the flow rate of the peristaltic pump and evaporation of the solvent are critical to the formation of colloidal crystals. In this case (the evaporation velocity $\sim 0.04 \mu\text{m} \cdot \text{s}^{-1}$), ethanol has to pass along a relative long distance during the self-assembly process. So the undulation originated from the evaporation of ethanol can not be observed. Moreover, the film derived from the FCVD is more homogeneous than those obtained from other methods. Even though the same initial concentration of silica has been used for the film depositions, the film thicknesses of the three samples are obviously quite different. For TCVD at 55°C the film is thicker than the one from NVD, while the opal film from the FCVD shows a very thin layer.

2.1.2 SEM images

Fig.2 shows the SEM top-view images of the colloidal crystal films fabricated from silica spheres of



(a) NVD, (b) TCVD (40°C), (c) TCVD (40°C), low magnification ($\times 1000$), (d) TCVD (55°C), (e) FCVD ($0.47 \mu\text{m} \cdot \text{s}^{-1}$), (f) FCVD ($0.93 \mu\text{m} \cdot \text{s}^{-1}$)

Fig.2 SEM images (top views) of the colloidal crystal films with diameter 400 nm made by different VD methods

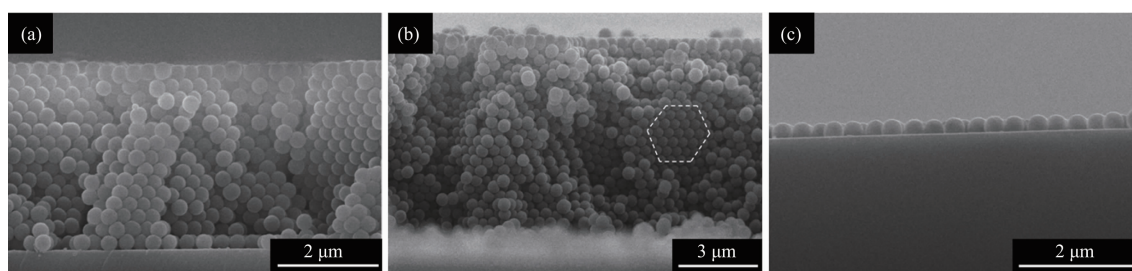
400 nm with different VD conditions. The samples are shown at low magnification in Fig.2 (c)~(d) to evaluate the effect of the evaporation temperature on the crystalline quality of colloidal photonic crystals. Meanwhile, SEM images of colloidal crystal films grown under various dropping velocity of liquid-surface are shown in Fig.2 (e)~(f). As a comparison, SEM image of silica film grown by NVD method at room temperature (25 °C) without relative motion of substrate is also shown in Fig.2(a).

It can be seen that the colloidal crystals exhibit a highly ordered structure with each sphere touching six others in one layer. The silica colloid arrangements are close-packed over a sample area up to 10 μm but tiny local defects can be found in Fig.2 (a) and (b), which are associated with the particle size variation. Fine cracks could be observed on the surface of the colloid film in the large domain with the increasing of temperature for rapid evaporation as shown in the low-magnification SEM images (Fig.2(c) and (d)). The appearance of these cracks is due to the release of the stress accumulated in the lattice due to shrinkage of spheres during the drying process.

Fig.2(e) and (f) indicate that the dropping velocity of the liquid-surface may seriously affect the quality of colloidal crystals. With the increase in dropping

velocity, films show different surface morphologies. When dropping velocity is increased beyond $0.47 \mu\text{m} \cdot \text{s}^{-1}$, the silica spheres do not have sufficient time to shift to favorite lattice sites during self-assembly, leading to the formation of defects, such as line dislocations. At dropping velocity of $0.93 \mu\text{m} \cdot \text{s}^{-1}$, the film shows an increased spacing between spheres, implying the loss of structural ordering.

Fig.3 shows the cross-sectional SEM images of the colloidal crystal films formed by 400 nm silica spheres with the same volume fraction. Different film thicknesses can be obtained by changing the VD method. Fig.3(a) shows the film fabricated using NVD method with a thickness of 15 layers ($\sim 4 \mu\text{m}$). We can see that the formation of thicker crystals is strongly favored when higher evaporation temperature is employed. Fig.3 (b) shows a film about 8 μm fabricated under evaporation temperature at 55 °C. Using the FCVD for colloidal crystal, under the dropping velocity of $0.70 \mu\text{m} \cdot \text{s}^{-1}$, a film with monolayer spheres is obtained, as shown in Fig.3 (c). From the comparison of the three methods, it can be seen that the higher temperature, the thicker the crystalline film attained, while the operation of peristaltic pump leads to the liquid surface withdrawn quickly and thus decrease the film thickness during self-assembly.



(a) NVD (25 °C), (b) TCVD (55 °C), marking indicates the hexagonal (111) planes. (c) FCVD ($0.70 \mu\text{m} \cdot \text{s}^{-1}$)

Fig.3 SEM images (cross-sectional views) of the colloidal crystal films with diameter 400 nm made by different VD methods

2.2 Optical properties

Although SEM is the best and most revealing method for evaluation of colloidal crystal perfection, it is necessary to further investigate the optical properties of the films, which can show the overall performance of the films in the presence of the defects such as line dislocations and microcracks. To optically characterize these structures, light transmission spectra of the

samples were measured at normal incidence in the wavelength ranging from 500 to 1300 nm using a UV-Vis-NIR spectrophotometer.

2.2.1 Influence of evaporation temperature

Fig.4 shows the transmission spectra of the as-prepared 3D colloidal photonic crystals grown from a 1.0% volume fraction solution at different evaporation temperatures. The black, red, and green lines

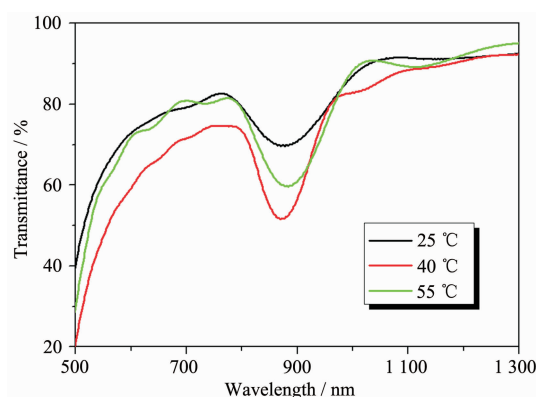


Fig.4 Normal incidence transmission spectra of samples grown from a 1.0% volume fraction solution at different evaporation temperatures

correspond to the samples fabricated at 25, 40, and 55 °C, respectively. The absorption maxima correspond to wavelength of 870 nm, 870 nm, and 884 nm, respectively. It must be noted that the absorption peak of the sample fabricated at 55 °C is red-shifted slightly. Theoretical calculations using Bragg law for normal incidence^[34] verify that the diffraction peak at wavelength of 884 nm corresponds to particle diameter of 400 nm for the face-centered (fcc) structure. As the evaporation temperature increasing, the Gibbs free energy difference between the fcc and hexagonal closely packed structure would increase^[35-36], thereby resulting in a preferential tendency towards the fcc phase.

The higher the evaporation temperature is, the shorter the self-assembling time, and this could minimize the particle sedimentation during VD process. For samples fabricated at a higher evaporation temperature, more silica nanospheres are deposited on the substrate, so the stop band is enhanced when raising the temperature from 25 to 40 °C. However, the evaporation temperature can not be too high. Faster evaporation rate increases the surface tension in thin colloidal film, leading to the formation of cracks in the 3D colloidal photonic crystals^[37]. So there is a trade-off between the desired optical quality and the time consumption. This is consistent with the previous SEM results shown in Fig.2 (c) ~ (d). Since the sample fabricated at 55 °C is less ordered with more cracks, its stop band is attenuated and broadened compared to that of the sample fabricated at 40 °C.

2.2.2 Influence of liquid surface dropping velocity

At the same time, different liquid surface dropping velocity has been tested for the self-assembly of silica particles. Fig.5 shows transmission spectra of samples grown under the liquid surface dropping velocity from 0.23 to 0.93 $\mu\text{m}\cdot\text{s}^{-1}$.

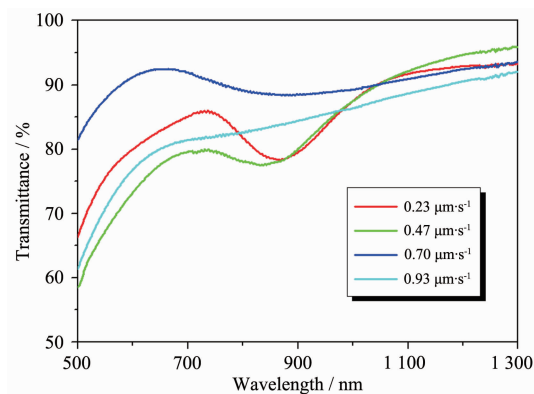


Fig.5 Normal incidence transmission spectra of samples grown from a 1.0% volume fraction solution with different pump flow velocities

A distinct transmission dip from Bragg diffraction of light has been observed around 870 nm under the liquid surface dropping velocity of 0.23 $\mu\text{m}\cdot\text{s}^{-1}$, suggesting that the particles are uniformly deposited. When the dropping velocity increases (0.47 $\mu\text{m}\cdot\text{s}^{-1}$), the stop band is broadened. We note that the absorption band vanishes when the dropping velocity exceeds 0.70 $\mu\text{m}\cdot\text{s}^{-1}$. The sample grown under this dropping velocity has no transmission dip due to the poor crystalline quality and small film thickness, as confirmed by SEM image of Fig.2 (f). Faster dropping velocity leads to random array formation, so the silica spheres do not have sufficient time to find suitable lattice sites, thus light diffraction effect is weakened^[38]. For the higher velocity ($>0.93 \mu\text{m}\cdot\text{s}^{-1}$), the substrate is not fully covered with particles, which is visible to the naked eye. To optimize the colloidal crystal quality and the time consumed, the value of liquid surface dropping velocity should never exceed 0.47 $\mu\text{m}\cdot\text{s}^{-1}$.

2.2.3 Influence of volume fraction

To fully exploit the potential of the improved VD method for photonic crystals preparation, the normal-incidence transmission spectra of silica colloidal crystal films obtained under 55 °C with different volume

fractions are also measured. The volume fraction used for fabrication varies from 0.25% to 2.0%. With increasing the volume fraction, the dips around 880 nm in the transmission spectra for 400 nm SiO₂ particles become narrow and the overall transmission drops as a result of the increase of film thickness, as shown in Fig. 6. Fabry-Pérot fringes originated from the finite film thickness can also be clearly observed, indicating the uniformity of film thickness over large areas. The corresponding transmission spectra confirm that the increase in the sharper attenuation dips of the stop band originates from an increase in efficiency of Bragg diffraction of light due to the larger number of lattice units present in thicker films.

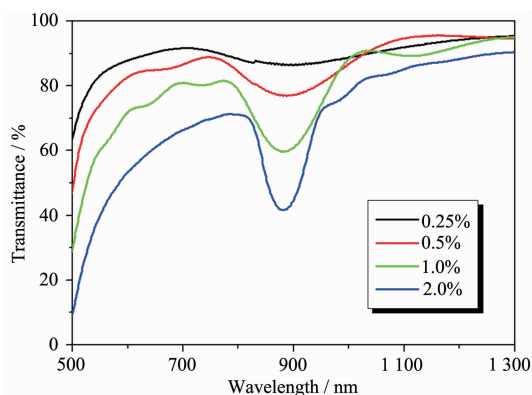


Fig.6 Normal incidence transmission spectra of samples grown under 55 °C with different volume fraction

The colloidal particles are deposited only at the air-water-substrate interface. To obtain colloidal crystals through the VD technique, a key point is to control the suspension surface dropping velocity. In Fig. 7, the three methods for large area colloidal crystallization are compared in terms of colloid consumption and fabrication speed. By NVD method, it generally takes several days to obtain colloidal crystals of 1 cm² area. With the help of variable-flow peristaltic pump, self-assembly process is quicker and easier to deposit monolayer of silica colloidal spheres onto the substrates, but a serious disadvantage of FCVD method is the inevitable large colloid consumption. Compared to the FCVD method in Fig.7, the TCVD method exhibits advantageous features of less consumption of colloids. Although the TCVD is slower than the FCVD method that usually requires concentrated suspensions

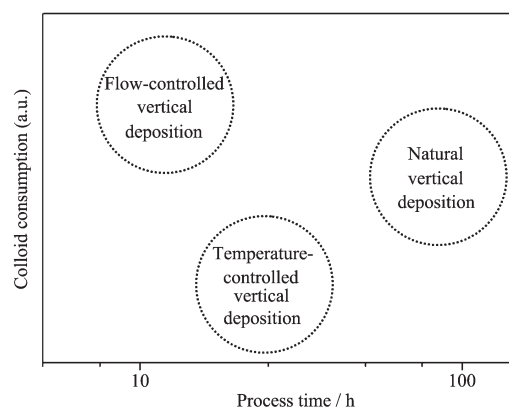


Fig.7 Comparison of different VD method for the fabrication of colloidal crystal films over large area

of particles, it is still much faster than NVD process. Therefore, in order to achieve thicker crystal easily and rapidly, high temperature of evaporation process and/or larger volume fractions of particles should be employed.

3 Conclusion

In conclusion, self-assembly of colloidal crystals from silica suspensions were studied by improved vertical depositions. The comparative study of three deposition methods on the array formation was conducted with microstructure analysis and optical transmission measurements. Results show that by increasing the rate of solvent evaporation or the relative movement between the liquid-surface and substrate, the problems of particle sedimentation associated with vertical deposition method can be minimized. Lower colloid consumption and shorter deposition time can be achieved through improvements by the TCVD method and the FCVD method, respectively.

References:

- [1] Ozin G A, Yang S M. *Adv. Funct. Mater.*, **2001**,**11**:95-104
- [2] Polman A, Wiltzius P. *MRS Bull.*, **2001**,**26**:608-613
- [3] Noda S. *Physica B*, **2000**,**279**:142-149
- [4] Blanco A, Chomski E, Grabtchak S, et al. *Nature*, **2000**,**405**: 437-440
- [5] Denkov N D, Velev O D, Kralchevsky P A, et al. *Langmuir*, **1992**,**8**:3183-3190
- [6] Cheng Z, Russell W B, Chaikin P M. *Nature*, **1999**,**401**:893-895

- [7] Miguez H, Meseguer F, López C, et al. *Adv. Mater.*, **1998**,**10**: 480-483
- [8] Wostyn K, Zhao Y X, Yee B, et al. *J. Chem. Phys.*, **2003**,**118**: 10752-10757
- [9] Jiang P, Ostojic G N, Narat R, et al. *Adv. Mater.*, **2001**,**13**: 389-393
- [10] Yamamoto T. *Appl. Phys. Express*, **2009**,**2**:101501
- [11] Vlasov Y A, Bo X Z, Sturm J C, et al. *Nature*, **2001**,**414**:289-293
- [12] Schaak R E, Cable R E, Leonard B M, et al. *Langmuir*, **2004**, **20**:7293-7297
- [13] Xu X X, Wang X, Nisar A, et al. *Adv. Mater.*, **2008**,**20**:3702-3708
- [14] Finkel N H, Prevo B G, Velev O D, et al. *Anal. Chem.*, **2005**, **77**:1088-1095
- [15] Wang L K, Zhao X S. *J. Phys. Chem. C*, **2007**,**111**:8538-8542
- [16] Jiang P, Bertone J F, Hwang K S, et al. *Chem. Mater.*, **1999**, **11**:2132-2140
- [17] Jiang P, McFarland M J. *J. Am. Chem. Soc.*, **2004**,**126**:13778-13786
- [18] Velev O D, Jede T A, Lobo R F, et al. *Chem. Mater.*, **1998**,**10**: 3597-3602
- [19] Park S H, Qin D, Xia Y. *Adv. Mater.*, **1998**,**10**:1028-1032
- [20] Im S H, Lim Y T, Suh D J, et al. *Adv. Mater.*, **2002**,**14**:1367-1369
- [21] Bardosova M, Pemble M E, Povey I M, et al. *Adv. Mater.*, **2010**,**22**:3104-3124
- [22] Grieseböck B, Egen M, Zentel R. *Chem. Mater.*, **2002**,**14**: 4023-4025
- [23] Cortalezzi M M, Colvin V, Wiesner M R. *J. Colloid Interface Sci.*, **2005**,**283**:366-372
- [24] Teh L K, Tan N K, Wong C C, et al. *Appl. Phys. A*, **2005**,**81**: 1399-1404
- [25] Chabanov A A, Jun Y, Norris D J. *Appl. Phys. Lett.*, **2004**,**84**: 3573-3575
- [26] Goldenberg L M, Jung B D, Wagner J. *Langmuir*, **2003**,**19**: 205-207
- [27] Gu Z Z, Fujishima A, Sato O. *Chem. Mater.*, **2002**,**14**:760-765
- [28] Zheng Z Y, Liu X Z, Luo Y H, et al. *Appl. Phys. Lett.*, **2007**,**90**:051910
- [29] Arsenault A, Fournier-Bidoz S, Hatton B, et al. *J. Mater. Chem.*, **2004**,**14**:781
- [30] Stöber W, Fink A, Bohn E. *J. Colloid Interface Sci.*, **1968**,**26**: 62-69
- [31] Bogush G H, Tracy M A, Zukoski C F. *J. Non-Cryst. Solids*, **1988**,**104**:95-106
- [32] Razink J J, Schlotter N E. *J. Non-Cryst. Solids*, **2007**,**353**: 2932-2933
- [33] Zhou Z C, Zhao X S. *Langmuir*, **2004**,**20**:1524-1526
- [34] Wang W, Gu B H, Liang L Y, et al. *J. Phys. Chem. B*, **2003**, **107**:12113-12117
- [35] Woodcock L V. *Nature*, **1997**,**385**:141-143
- [36] Deng T S, Zhang J Y, Zhu K T, et al. *Colloids and Surfaces A: Physicochem. Eng. Aspects*, **2010**,**356**:104-111
- [37] Ye Y H, LeBlanc F, Haché A, et al. *Appl. Phys. Lett.*, **2001**, **78**:52-54
- [38] Dux C, Versmold H. *Phys. Rev. Lett.*, **1997**,**78**:1811-1814